



# Erosive wear behavior of bio-waste particulate-reinforced epoxy composites for low cost applications

Prajapati Naik<sup>1</sup> · Prasanta Sahoo<sup>1</sup> · S. K. Acharya<sup>2</sup> · Smitirupa Pradhan<sup>3</sup>

Received: 31 May 2020 / Accepted: 12 November 2020 / Published online: 15 March 2021  
© Indian Academy of Wood Science 2021

**Abstract** Polymer based substances such as epoxy or poly-epoxide has tremendous role in industrial applications such as surface coatings, potting, laminated circuit boards due to its versatile nature. Synthetic fibers are used in polymer composites as reinforcement to increase its mechanical and tribological properties. However, natural fibers/particulates are more preferable over synthetic fibers due to their environment friendliness, high abundance, viable and cost effective. Due to easy accessibility and manufacturing, worldwide researchers have been tempted to develop biofiber-based composite material and study their ability in tribological applications. In this research paper, the erosive behaviors of reinforced epoxy composite with different weight percentage of bio waste (orange peel) were studied. The erosive wear behavior of fabricated composites was evaluated at different impingement/impact angles (i.e., 30°, 60°, 45° and 90°) and impact velocities (48, 70 and 82 m/s) with constant feed rate at 5 gm/min. The solid particle erosion was carried out taking silica sand as erodent and the average size of erodent is 150–250 µm. The impact velocity and impact angle have a tremendous effect on erosive wear. SEM study of eroded surfaces also carried out to inspect the worn surface morphology.

**Keywords** Natural fiber · SEM · Erosion wear · Reinforced composite · Silica sand · Impact angle

## Introduction

In nineteenth century, the human beings used metals and alloys for all most all applications. The metals and alloys are single phase and multiphase materials, respectively. However, due to high cost in extraction to production, complicated product design and ultimately disposal issues (waste materials), researchers developed a new set of two-phase material called composites. It contains a reinforcing agent which offers strength to composite material and an enfold matrix gives stability to the reinforcement phase. Natural or synthetic fibers can be reinforced into the polymeric resins (matrix) to synthesize the composite materials as per specific requirements from the industries. The major synthetic fibers, used to synthesize composite materials are glass (Sathishkumar et al. 2014), carbon (Bhatt et al. 2017), Kevlar (Dong et al. 2018), graphite (Knoell et al. 1975), etc. However, these synthetic fibers are non-biodegradable. The whole world is now facing lots of environmental issues. So the scientists and engineers are looking environmental friendly materials for various applications. Nowadays, conventional synthetic fibers are substituted by natural fibers for various applications such as house hold applications, automobile parts, sports kits, structures, and marine applications due to their abundant availability, cost effective, high strength, resistance to corrosion, etc. (Bharath et al. 2016; Fragassa et al. 2017; Adesina et al. 2019; Santos 2009; Amiandamhen et al. 2016). The biofibers are also in demand because of low density, outstanding stiffness, and reduced energy consumption during production, non-irritation to skin and good

✉ Prajapati Naik  
pnayakcet@gmail.com

<sup>1</sup> Faculty of Engineering and Technology, Jadavpur University, Kolkata, West Bengal, India

<sup>2</sup> Mechanical Engineering Department, NIT Rourkela, Odisha, India

<sup>3</sup> Mechanical Engineering Department, KITS University, Bhubaneswar, Odisha, India

thermo-mechanical properties, particularly from many traditional engineering materials such as metals and alloys (Gholampour et al. 2020; Peças et al. 2018; Mohammed et al. 2015; Sanjay et al. 2016; Mahesh et al. 2019). Several researchers reported that the plant base bio-waste materials such as coir (Verma et al. 2013), sisal (Munde et al. 2019), jute (Kumar et al. 2017), flax (Fouk et al. 2010), hemp (Shahzad et al. 2012), kenaf (Haniffah et al. 2015), bamboo (Gupta et al. 2011) are the potential reinforcement instead of synthetic fiber in composite industries. Wood plastic composites are now in use for various outdoor applications such as building products, automotive and structural applications. As building products their use is found in decking, fencing, doors and window panels, roofing tiles, etc. The cost and availability of wood sometimes restricts their use. The present composite could be a substitute to WPCs with improved performance and give way to agro waste utilization.

Erosive wear (EW) behavior of the composite is the most important tribological problems faced by different industrial sectors. It occurs when hard particles are entrapped in air and strikes the specimen at different impingement angles. Subsequently, the material is removed from the surface of the specimen. This type of material loss is one of the most important failures in material industries. Researchers reported that the EW behavior depends upon the size and quality of erodent material, mass flow rate of erodent, air velocity and impact angle (Xie et al. 2016; Stachowiak et al. 1994; Sundararajan et al. 1990). Some of the machineries in various applications such as wind mill blades, water pipes, aero plane wings, blades of helicopter rotor and pump impeller are prone to erosive wear. Thus, the study of erosive wear behavior is vital as not only it changes the surface of the specimen but also changes the properties of the component.

The EW behavior is mostly occurred in the desert environment due to its sandy nature. Number of materials are engaged in desert environment, preferable polymer based composite materials. The polymer composites are also used in several sectors, especially in tribo-applications where liquid lubricants cannot be used due to different constraints (Bijwe and Fahim 2000; Rajesh et al. 2001). The main focus is to diminish wear as the cost of replacing worn parts is more expensive in most of the applications.

The EW behaviors of natural fiber based composites have been reported by several researchers in different literatures. Depending upon the nature of the material (ductile, semi ductile or brittle), the behavior of EW varies (Barkoula et al. 2002). The EW of composite specimen depends upon various factors such as type of filler material, impact angle, erodent velocity, size of the filler and the standoff distance (Pool et al. 1986; Xie et al. 2016; Pour-saeidi et al. 2017; Harrsha et al. 2007). Panchal et al.

(2018) analyzed the EW of epoxy composites incorporated with boiled and unboiled egg shell particulates. They found that unboiled egg shell particulate-reinforced epoxy composites shows better EW resistance than boiled egg shell-based composites. Shakuntala et al. (2014) investigated the mechanical and wear behavior of epoxy composites adding wood apple particulate as a filler material. They noticed that the mechanical behavior and EW resistance of synthesized composite specimen increase significantly by incorporating filler material. They also observed that maximum erosion occurs in between 45° and 60° for all the fabricated composite samples under consideration. Gupta et al. (2011) studied the EW behavior of bamboo epoxy composite material. They found that due to addition of bamboo fiber, the maximum erosion occurs at impact angle in between 60° to 75°, which shows the semi brittle nature of developed composites. Rout and Satapathy (2012) investigated the EW behavior of rice husk (RH)-based polymer composites and observed that RH act as a barrier against EW behavior. They also noticed that the developed composite materials absorb the part of kinetic energy of erodent particles and delay the exposure of the fiber. Srivastava et al. (2006) studied EW behavior of wheat flour filled glass epoxy composites and found that due to better bonding strength between filler material and glass fiber, the fabricated filled composite materials have better wear resistance as compared to un filled composites. Pani et al. (2019) studied the physical, mechanical and EW behavior of waste bagasee based composites where they observed that weight percentage of fiber, impact velocity and impingement angle are the main controlling factor in the EW analysis. They also reported that the standoff distance has least effect on the EW analysis. EW behavior of date palm leaf fiber-based polyvinylpyrrolidone composite has been studied by Mohanty (2017). He reported that impingement angle has strong influence on erosive wear analysis in comparison to impact velocity. However, a very few researchers have highlighted the tribological behavior of fruit waste.

The EW of natural fiber-based composite material was studied by several researchers at different operating conditions. Solid particle EW behavior was investigated on glass fiber epoxy composites with and without addition of egg shell materials with dimension  $100 \pm 15$  microns, where alumina ( $Al_2O_3$ ) act as erodent. The researchers found that impact velocity (erodent flow rate) is more responsible toward material removal rate as comprised to impact angle (Khan et al. (2019). Mishra et al. (2010) studied the influences of different impact angles and impact velocities on EW behavior of Bagasses fiber-reinforced polymer composites. Deo et al. (2009) investigated the EW behavior of the Lantana-Camera fiber-reinforced matrix composite with particles size of silica sand is  $200 \pm 50 \mu m$

which acts as an erodent. Biswas et al. (2012) studied the EW behavior of Bamboo and glass fiber hybrid-reinforced epoxy composite using hand-layup technique. Several authors (Raghavendra et al. 2014; Majumdar 2016; Prakash et al. 2020) observed that the tribological behavior of natural fibers such as jute fiber gives better performance as compared to glass and neat epoxy reinforced epoxy composites.

Ojha et al. (2012) investigated the properties of polymer composites using orange peel particulate as the filler material. They reported that the mechanical properties of developed composite increase with addition of filler loadings. From SEM, they also noticed that the addition of OPP increases bonding between matrix and filler materials. Rathinavel et al. (2020) also studied the mechanical behavior of polyvinyl alcohol/orange peel powder bio composite films. They observed that the tensile properties increase with increase in filler loadings. However, no literature available on the wear behavior of OPP based composites. In this paper, the different weight percentage of bio-waste (orange peel particulate) was reinforced with epoxy resin to fabricate the composite specimens as a replacement of non-biodegradable polymer material in various industrial applications. The prime focus of this work is to fabricate composite specimen with OPP as a filler material and epoxy as the matrix with varying OPP filler percentage likely 5%, 10%, 15% and 20% and study the EW behavior of developed composite specimens under various experimental conditions. The developed composite material containing 5%, 10%, 15% and 20% filler material is represented as OP1, OP2, OP3 and OP4, respectively. The experimental results are also analyzed using scanning electron microscope (SEM).

The present article contains four sections: the experimental work explaining the experimental setup, materials and approach used is explained in “[Materials and methods](#)” section followed by introduction, the description of the results followed by SEM analysis is represented in “[Results and discussion](#)” section and finally conclusion is in “[Conclusions](#)” section.

## Materials and methods

### Raw materials

The epoxy resin (Araldite LY-556) was used in the present study. It comprised of three-member ring structure, which contains two carbon atoms and an oxygen atom. The first product from the liquid reaction of bisphenol-A, is epoxy resin and its chemical name is Diglycidyl-Ether of Bisphenol-A (DGEBA). In comparison to other resins (thermo-set or thermoplastic), epoxy resins are widely used

in industrial applications due to its useful properties such as low shrinkage during cure, good moisture resistance, excellent chemical resistance, good electrical and mechanical properties (Reis et al. 2015). The density and viscosity of epoxy resin are  $1200 \text{ kg/m}^3$  and  $(11-14) \times 10^6 \text{ kPa}$  at room temperature, respectively. The hardener HY-951 chemically known as 2-ami-neethylethane-1, 2-diamin was applied to cure epoxy resin. The hardener is used to create strong cross-linked molecular structures that possess good strength, toughness and virtual impermeability in the cured film.

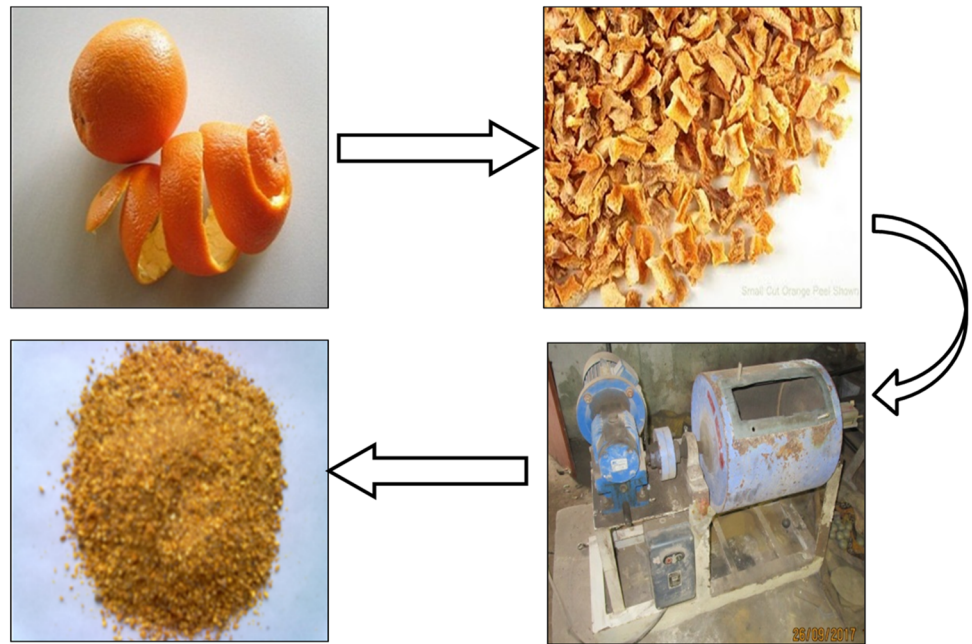
Citrus Aurantium Dulcis (CAD) is the scientific name of orange, is a species of citrus tree grown around the world. North eastern India, southern China and Indonesia are the countries where oranges are cultivated initially. This is a widely used fruit after banana and mango in India. Consumption of orange is also very high in all over India. The outer surface of orange is orange peels (OP). Previously, these are mostly used for land filling, animal feeding and composting. Later on, researchers realized the importance of the biological volume of this waste and tried to make use of this waste which possess many medicinal properties such as for glowing skin, unclog skin pores, treat pimples and acne, reduce inflammation. However, every year a major share of this waste material was used for the purpose of dumping which causes both socioeconomic and ecological problems such as high transportation cost, lack of dumping site, and accumulation of high organic content material. Therefore, researchers tried to develop the more effective and sustainable methods for utilization of this waste materials; OPP act as a filler material in composite industries for the production of lightweight composite materials.

Orange peels used in this research work was collected from local market and cleaned with distilled water to eradicate the unwanted particles. Then, the OPP materials dried in an oven at  $100 \text{ }^\circ\text{C}$  for two hours to eradicate the moisture. After complete drying, the particles were grinded to fine powder by ball milling machine. The particle size,  $1-212 \text{ }\mu\text{m}$  was used for the experimental purpose through Sieve analysis. The details of the preparation of OPP from orange peels are presented in Fig. 1.

### Fabrication of bio-composite

The wooden mold of size  $150 \text{ mm} \times 65 \text{ mm} \times 5 \text{ mm}$  was prepared for the fabrication of composite plate. The composite plates were fabricated with epoxy and OPP as a matrix and reinforcement, respectively. During the fabrication of composite plate the weight percentage of filler material was varied from 0 to 20%. The weight percentage (wt%) of the material (reinforced) was estimated using Eq. (1).

**Fig. 1** Procedure for OPP preparation



Weight % of reinforcement

$$= \frac{\text{Weight of reinforcement}}{\text{Weight of reinforcement} + \text{Weight of epoxy}} \times 100 \quad (1)$$

In this research work, hand layup technique was incorporated for the fabrication of composite plate. The mold used for the purpose of fabrication is shown in Fig. 2. In the bed of wooden pattern, a pattern removal sheet was positioned and also pattern discharge spray was used on the inner side of pattern for speedy and easy removal of fabricated specimen. The epoxy resin and hardener in the ratio 10:1 by weight mixed meticulously in a container at ambient conditions to manufacture composite specimens of different weight percentage of filler material. The mixture was then poured into the prepared mold. For elimination of

air bubbles and uniform distribution of the mixture of the pattern, a roller was rolled for two to five minutes. After that, the pattern free sheet was placed on the top of the pattern. A wooden plate of required dimension was kept in the mold and loaded with dead weights before the reaction starts and the mixture gets hardened. The pattern is under observation for 48 h. During the experiment, care should be taken to get uniform thickness because due to appliance off load, some mixture may be squeezed out from the pattern. After specifying the observation time the specimens were taken out from the mold. The composite samples were cut for different experimental purpose as per ASTM standard from the composite slab. After that, the samples were kept in an airtight container for further experimental purpose. Care should be taken so that the samples should not contact with moisture.



**Fig. 2** Wooden mold for fabrication of composite

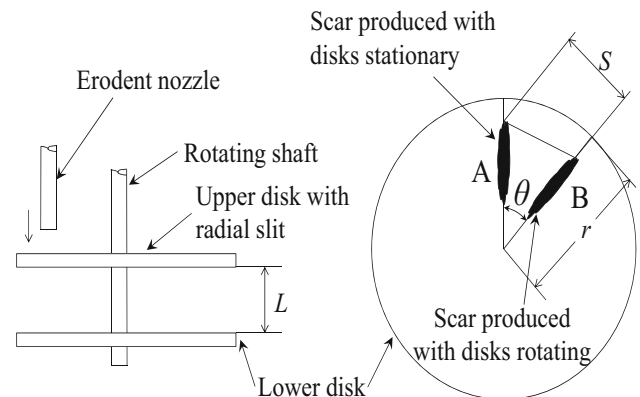


**Fig. 3** Line diagram of rotating double disk method for measuring impact velocity



**Impact velocity of erodent particles: rotating double disk method**

The erodent particle velocity (impact velocity) is measured by rotating double disk method (Fig. 3) which is widely accepted (Ruff et al. 1975). In double disk method, the two disks are mounted on a common shaft. A thin radial slot cut in the upper disk and the lower disk coated with a thin paint or dye film to mark the position of striking particles. Two erosion scars are formed at an angular displacement of  $\theta$  and linear distance  $S$  between stationary disk and rotational disk (rotates with prescribed velocity). The angular displacement is used to determine the time required for the particles to travel the distance  $L$  which is the distance between the disks.

The velocity of the particle ( $V$ ) can be evaluated using Eq. (2).

$$V = \frac{L}{t} = 360^\circ \left( \frac{L\omega}{\theta} \right), \tag{2}$$

The expression for  $V$  can also be expressed as by using Eq. (3)

$$V = \frac{2\pi r\omega L}{S} \tag{3}$$

$r$  represents the rotating disk radius and  $\omega$  is the angular velocity. The calibrations of impact velocity at different pressures (1 bar, 2 bar and 3 bar) are presented in Table 1.

**Fourier transform infrared spectroscopy (FTIR)**

To study the structure of inter and intra-molecular hydrogen bonding in cellulose, FTIR approach is generally used. The detailed analysis gives a relationship between the nature of hydrogen bond and physical and mechanical

properties of cellulose. This analysis was conducted by using IR-prestege-21 spectrometer where hundred scans were taken in the range 400–4000  $\text{cm}^{-1}$  wave numbers with resolution rate 2  $\text{cm}^{-1}$ .

**Surface hardness**

The hardness of the developed specimens can be calculated by Lecco Vickers Hardness (LV 700) device. A diamond indenter of square base right pyramid was forced into the material under load. The angle between the opposite faces is 136°. Equation (4) is used to calculate the Vickers hardness number of developed composites.

$$H_v = \frac{0.1889F}{D^2}, \tag{4}$$

where  $F$  the applied load to the specimen (kgF) is,  $D = (D_1 + D_2)/2$  is the mean value of  $D_1$  (indentation in horizontal direction (mm)) and  $D_2$  [indentation in vertical direction (mm)].

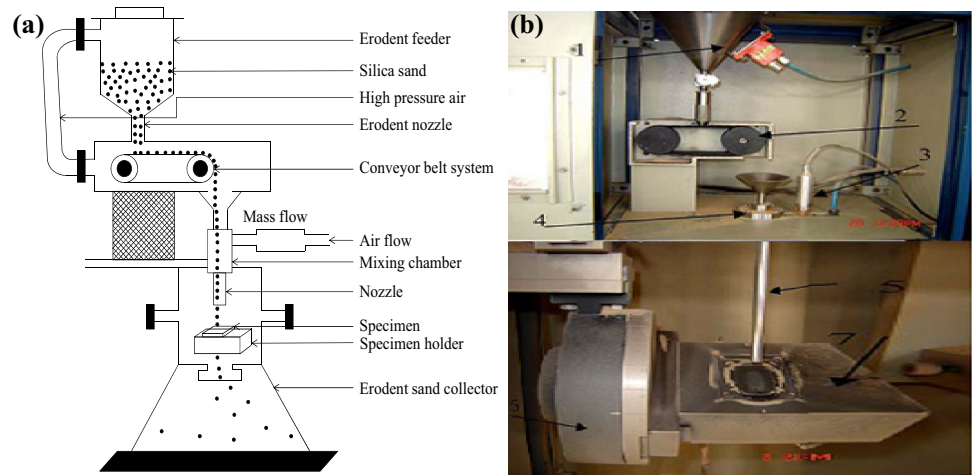
**Wear test and measurement**

ASTM G76 standard was used to study the EW behavior of synthesized specimens on the erosion test rig. The line diagram and actual test rig, both are presented in Fig. 4. The test rig consists of different parts such as 1-sand hopper, 2-conveyor belt system, 3-pressure transducer, 4-mixing chamber, 5-nozzle, 6-X-Y and  $h$  axes assemble, 7-sample holder (as mentioned in actual test rig). The silica sand of size 150–250  $\mu\text{m}$  was mixed with air (compressed and dried) continuously in the mixing chamber through conveyor belt feeder. The fabricated specimens with dimension 30 mm  $\times$  30 mm  $\times$  3 mm were kept at different impingement angles such as 30°, 45°, 60° and 90°

**Table 1** Calibration of erodent flow (impact velocity)

Pressure (bar)	Rotating disk velocity (rpm)	Angle (°)	Velocity of erodent particle (m/s)	Impact velocity (avg.) (m/s)
1	2000	7.0	42.85	47.25
		6.5	46.15	
		6.0	50.00	
		6.0	50.00	
2	2000	4.0	75.00	69.16
		4.5	66.67	
		4.0	75.00	
		5.0	60.00	
		4.5	66.67	
3	2000	4.5	66.67	81.845
		4.0	75.00	
		3.5	85.71	
		3.0	100.00	

**Fig. 4** Erosion experimental test rig. **a** Line diagram. **b** Actual machine



with respect to the trajectory of sand particles. The silica particles were passed through a 4 mm diameter tungsten carbide converging nozzle. After passing through the nozzle, the silica particles were accelerated and bombarded to the target material. During bombardment, the standoff distance (distance between target material and nozzle) was kept constant throughout the experiment i.e., 10 mm. The impact velocity of erodent was varied by varying the pressure of compressed air and it was evaluated by using rotating double disk method as explained in the “[Impact velocity of erodent particles: rotating double disk method](#)” section.

Generally the EW behavior was determined by the weight loss method. Prior to experiment, the tested specimens were washed with acetone. The fine sand particles adhere to the composite surfaces were removed from by a brush. Subsequently, the surface was cleaned with acetone soaked cotton material to eliminate the wear debris for further use. The erosion wear rate ( $E_r$ ) is then calculated by using Eq. (5).

$$E_r = \frac{\Delta w}{w_e}, \quad (5)$$

where  $\Delta w$  is the weight loss of tested samples (gm) and  $w_e$  is the total weight of erodent used.  $\Delta w$  was evaluated using an electrical weighing machine with accuracy 0.001 mg by weighting the tested specimen before and after each experiment. This process was repeated until the steady state erosion attained. The erosion test parameters are presented in Table 2. The erosion tests are generally carried out at normal atmospheric conditions. If the temperature of erodent particles is increased, the target specimen dissipates large amount of energy in the form of thermal energy and kinetic energy. That causes severe damage to target material (Shimizu et al. 2011).

**Table 2** Detailed design parameters for the experimental study

Test parameters	
Erodent	Angular silica sand
Erodent size	150–280 $\mu\text{m}$
Impact angle	30°, 45°, 60° and 90°
Impact velocity	48 m/s, 70 m/s and 82 m/s
Feed rate	5 gm/min
Experimental temperature	Normal atmospheric temperature
Standoff distance	.1 cm
Diameter of nozzle	0.04 cm
Time	60 s

### SEM analysis

SEM was used to study the morphological analysis of raw and CB powders as well as tested samples. SEM analysis was carried out at 15 kV accelerating voltage by using the Nova Nano SEM450 device. To improve the conductivity of the samples before taking the micrographs, a thin film of platinum was vacuum-evaporated onto them.

## Results and discussion

### FTIR analysis

The FTIR analysis of the OPP material was carried out to set up a bond between the functional group and its vibration frequency change. Figure 5 represents the FTIR analysis of the OPP material. It reveals the presence free hydroxyl groups as the absorption peak observed around  $2320.31 \text{ cm}^{-1}$ . In OPP, the C-H stretching, the existence of alkane functional group was observed because the vibration frequency changes in the region of  $2425.81 \text{ cm}^{-1}$ .

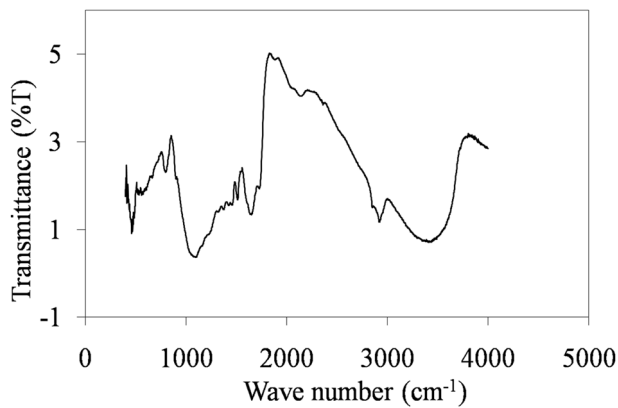


**Fig. 5** FTIR spectroscopy of OPP

The absorption peaks are in the range  $1641.31\text{--}1737.74\text{ cm}^{-1}$  which matches with C=O stretching due to the presence of aromatic groups such as lignin and hemicelluloses. The C=C stretching vibrations in the region of  $1546.8\text{--}1652.88\text{ cm}^{-1}$  indicate the existence of alkenes and aromatic I groups. The presence of CH<sub>2</sub> and CH<sub>3</sub> groups were observed at the absorption peak of  $1461.94\text{ cm}^{-1}$ , while peak at  $1380\text{ cm}^{-1}$  is observed due to the presence of CH<sub>3</sub> group. The peaks at  $1379\text{ cm}^{-1}$  and  $1153.35\text{--}1300\text{ cm}^{-1}$  may be due to the existence of aromatic CH and carboxyl-carbonate groups and vibration of CO groups, respectively. The peaks at  $476.38\text{--}862.12\text{ cm}^{-1}$ ,  $1080.06\text{ cm}^{-1}$  and  $1238.21\text{ cm}^{-1}$  is due to Si–H group, CH–OH stretching and Si–O–Si stretching, respectively.

### Hardness test

The property of composite material which resists scratching, indentation, penetration and plastic deformation is known as hardness. The surface hardness is one of the significant parameters that govern the EW resistance. The surface hardness of fabricated composite specimens

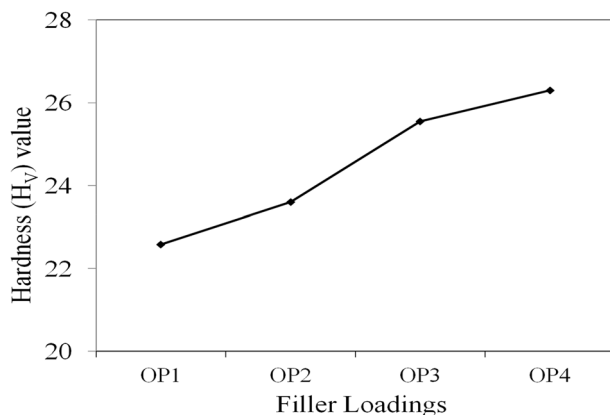


**Fig. 6** Surface hardness of composite specimen

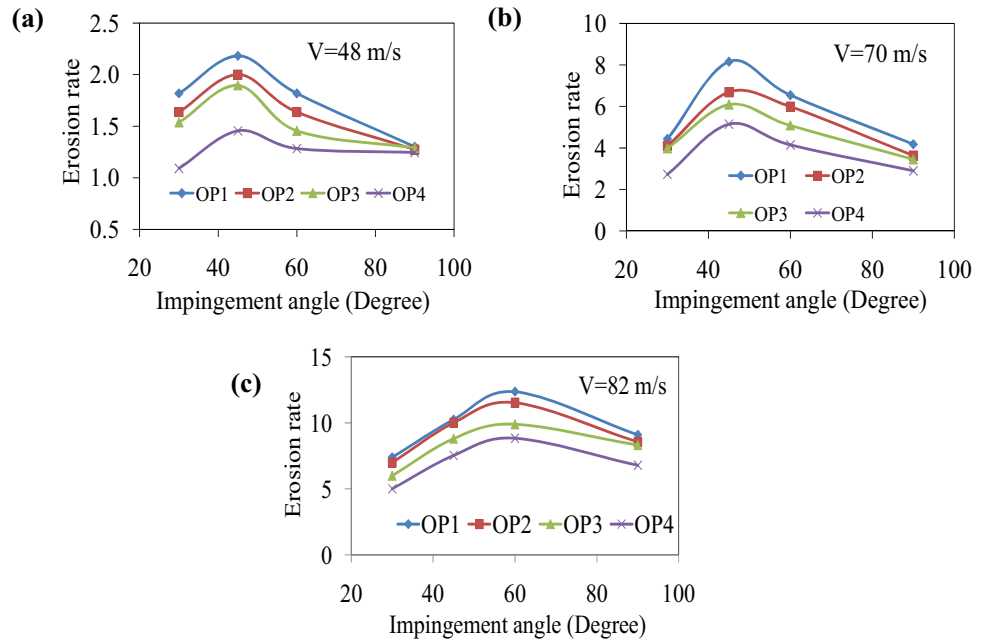
(different weight percentage) is presented in Fig. 6. It is noticed that the surface hardness of developed composite material increases with increasing the weight percentage of filler materials. However the increment of hardness is marginal. The reason is that hardness of composite material depends upon of relative fiber volume and modulus (Ferrigno et al. 1978).

### Influence of impact angle ( $\alpha$ ) on EW performance of OPP composite

Several researchers reported that impact angle (angle between erodent trajectory and target specimen) is one of the significant factors to evaluate the erosive behavior of composite specimens. The impact angle was also used to study the nature of the material i.e., brittle or ductile using the relationship of impingement angle and erosion rate. The material indicates ductile nature and brittle nature if the maximum erosion develops at low impact angle ( $15^\circ < \alpha < 30^\circ$ ) and normal impact ( $\theta = 90^\circ$ ), respectively. The erosion wear behavior of composite specimen increases due to impact angle (Pool et al. 1986). The impact of impingement angle of synthesizes specimens on EW at different impact velocities is presented in Fig. 7.

Studies reported that that maximum EW ( $E_{rmax}$ ) occurs at normal impact ( $\alpha = 90^\circ$ ) for neat epoxy composites which shows brittle behavior of epoxy material. However, in this investigation, the maximum erosion was noticed at  $45^\circ$  impact angle irrespective of the weight percentage of filler loadings for low impact speed, i.e., 48 m/s and 70 m/s and in case of higher impact velocity (82 m/s) the maximum value is observed at  $60^\circ$  impingement angle. The minimum EW rate ( $E_{rmin}$ ) is observed at low impact angle ( $30^\circ$ ) for all synthesise composite specimens under all impingement velocities. In the present investigation, it is observed that, the developed composite materials were changed their behavior from pure brittle to semi ductile nature at low impact velocities due to addition of OPP filler materials. However, for higher velocity the nature tends toward semi brittle. This indicates the benefit of addition of OPP to pure epoxy. Further, it is also observed from these plots that OP4 composite shows maximum wear resistance irrespective of the impact velocities. So from the above analysis it has been observed that the OPP-reinforced composite specimens show signs of semi-ductility, since peak erosive wear observed at the intermediate impact angles of ( $45^\circ < \alpha < 60^\circ$ ). Studies reported that the wear properties polymer composites (either progress or failure) are greatly depend upon the interaction phenomenon matrix and filler particles (Li and Sheng 2010). However, in this experimental work it has been observed that the incorporation of OPP filler material increases the wear

**Fig. 7** EW behavior of OPP composites at different impact angles and different velocities: **a** 48 m/s. **b** 70 m/s. **c** 82 m/s



resistance of polymer composites. This is attributed to good interaction between OPP filler and matrix material.

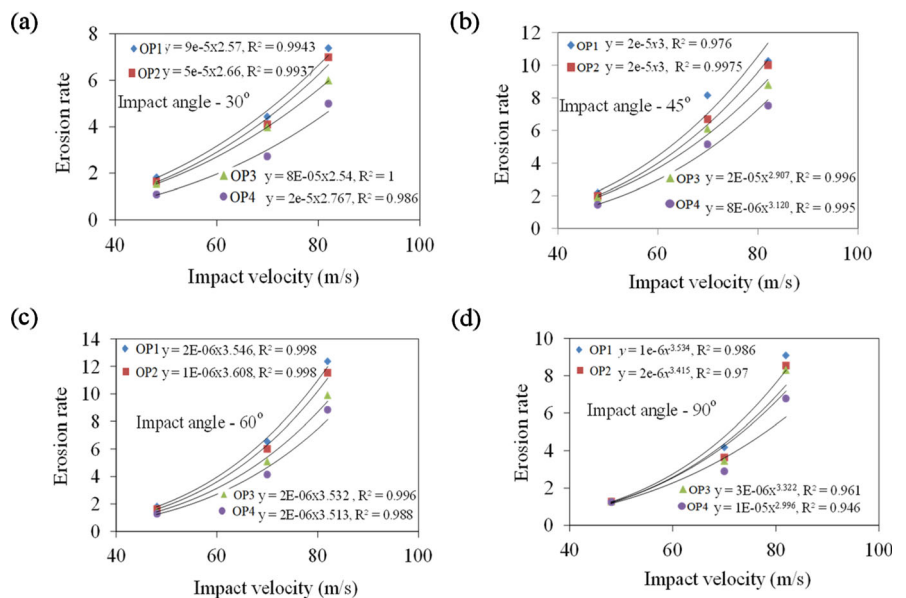
**Influence of impact velocity on EW of OPP composite**

The impact or impingement velocity (the velocity with which erodent particle strikes the target material) of erodent particle has a powerful influence on the EW process. EW develops in the material, due to increase in impact velocity and their impact energy. Figure 8 represents the erosive wear behavior of all specimens at different impact

velocities and different impact angles. From the graphs it has been observed that there is no major alteration of erosive wear at low impact velocity ( $\cong 48\text{ m/s}$ ). At low impact velocity, stresses developed due to impact velocity are very less for plastic deformation. On the other hand surface fatigue is the reason for the material removal (erosive wear) at low impact velocity. Hence low impact velocity is considered as quasi-static process.

However, the erosive wear behavior enhanced considerably due to improve of impingement velocities. In this cases, the eroded specimen experiences plastic deformation at impact point which leads to higher amount of material

**Fig. 8** EW of OPP composites at different impact velocity for different impingement angles **a** 30°. **b** 45°. **c** 60°. **d** 90°





removal. The similar results also reported by several authors while studying natural fiber-reinforced composite materials (Khan et al. 2019; Jena et al. 2018). Cracking also observed at the subsurface of erodent specimen due to impact of erodent. Studies reported that the rate of erosive wear for steady state condition can be formulated as  $E = Kv^n$ , where  $E$  is the EW rate,  $v$  is the impact velocity,  $n$  is the velocity exponent and  $K$  is an empirical constant (Stachowiak et al. 1994). The velocity exponent is calculated by erodent and target material characteristics. From the graphs, it has been observed that the velocity exponent varies in between 2.57 to 3.532. From the literature it is observed that the value of  $n$  varies from 2 to 3 for polymeric material behaving ductile nature and from 3 to 5 for brittle material. However from the graph it is concluded that the developed material is semi ductile nature.

### Erosion efficiency

Erosion efficiency ( $\eta$ ) is the ratio between volumes of material (actual) detached as erosion debris to the displaced volume and is presented in Eq. (6) (Sundarajan et al. 1990).

$$\eta = \frac{2E_r H_T}{\rho v^2}, \quad (6)$$

$E_r$  is erosive wear rate (kg/kg), the hardness of targeting materials is  $H_T$  (MPa), density of the targeting material is  $\rho$  (kg/m<sup>3</sup>) and  $V$  is the impingement speed (m/s). The erosion efficiency indicates the character of erosive wear mechanism. If the erosion efficiency is zero, then EW had taken place on the surface of the specimen due to ideal ploughing without development of any fracture. On the other hand if  $\eta$  value is one or 100% then removal of material due to micro cutting. Erosive wear efficiency ( $\eta$ ) is greater than one for brittle materials and much less than one for ductile materials. In case of brittle material the erosive wear is due to breaking of fragments which is the reason for the formation and interlinking of cracks. However erosive wear of ductile material is possible due to repetitive impingement of eroding particles. The values of erosion efficiency of synthesize specimens filled with different doses of OPP filler are calculated and presented in Table 3. From this investigation it has been observed that OP4 composites show lower value of erosion efficiency. It has been already discussed that the OP4 composites indicate exceptional erosive resistance in comparison to other fabricated specimens. That shows, the composite specimens have lower  $\eta$  indicate exceptional erosion resistance whereas higher values of  $\eta$  show poor resistance to erosion mechanism. Pani et al. 2019 estimated the erosive wear efficiency of iron-mud reinforced glass fiber polymer composite and found similar behavior. However, Srivasatav et al. (2006) found decrease in erosive wear efficiency with increase of

impact velocity while studying fly ash filled glass fiber polymer composites. Since the results obtained from the literature regarding relation between erosive wear and erosion efficiency are different from analysis to analysis, so it is concluded that the wear efficiency not only depends upon the impact velocity but also depends upon type of filler materials. The erosion efficiencies of synthesize OPP composites vary from 2.247 to 4.579 and 1.982 to 5.281 at an impingement angle of 45° and 60°, respectively, for considered impact velocities. Considering the results of wear efficiency ( $\eta$ ) and velocity exponent ( $n$ ), the synthesize composite can be treated as semi ductile material. In the paragraph 3.2, the author also concluded that the fabricated specimen is semi ductile nature.

### Effect of Filler loadings

Initially the filler materials are added to the composite materials, to decrease the cost of the materials but as time progressed fillers are used to enhance the tribological and mechanical properties. The effects of filler material on the EW (weight loss) of the developed specimens at different impact velocities are presented in Fig. 9. It has been noticed that the augmentation of OPP filler material improves the wear resistance of the composite specimens i.e., the material removal rate decreases in all impact velocities. The minimum weight loss was observed in case of OP4 composite specimens because the incorporation of filler materials leads to adequate interfacial bonding with matrix material. Further it is observed that there is a 25% decrease in weight loss of OP4 specimen in comparison to OP1 composite specimen at low impact velocity (48 m/s) and 45° impact angle. Similarly the weight loss of OP4 specimen is 28% in comparison to OP1 composites at high impact velocity (82 m/s) at same impact angle. So it clearly recognizes the impact of OPP filler on EW. It is also seen that the weight loss of specimen increases with increase in impact velocities due to gradual increase in material removal rate with impact velocities. This is because the temperature develops at the intermediated region due to increase of impact velocity that degenerate the interfacial bonding and thereby causing material removal.

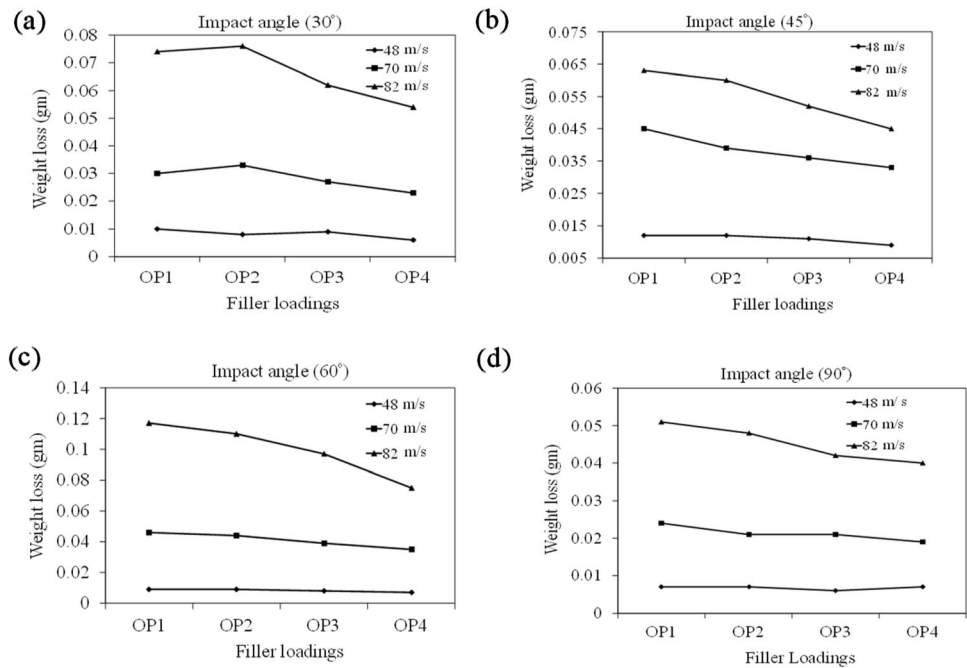
### Study of surface morphology

To investigate the surface morphology and analyze EW mechanism, the eroded specimens were studied under SEM.

The surface morphology of eroded surface [at 48 m/s (impact velocity), 30° (impact angle)] is presented in Fig. 10a. It has been noticed that the impact of erodent particle on the surface of composite specimen (OP4) is very less.

**Table 3** Values of  $\eta$  for different OPP composites

Impact velocity (m/s)	Impact angle (°)	Erosion efficiency( $\eta$ )			
		OP1 $H_V$	OP2 $H_V$	OP3 $H_V$	OP4 $H_V$
		22.58	23.6	25.55	26.3
48	30	2.134	2.188	1.99	1.685
	45	2.561	2.674	2.457	2.247
	60	2.134	2.188	1.885	1.982
	90	1.526	1.702	1.670	1.923
70	30	2.449	2.578	2.426	1.981
	45	4.506	4.206	3.712	3.737
	60	3.613	3.772	3.102	3.011
	90	2.308	2.286	2.105	2.103
82	30	2.969	3.200	2.664	2.646
	45	4.125	4.579	3.908	3.984
	60	4.973	5.281	4.394	4.677
	90	3.657	3.915	3.287	3.589

**Fig. 9** Effect of filler on weight loss of fabricated specimens

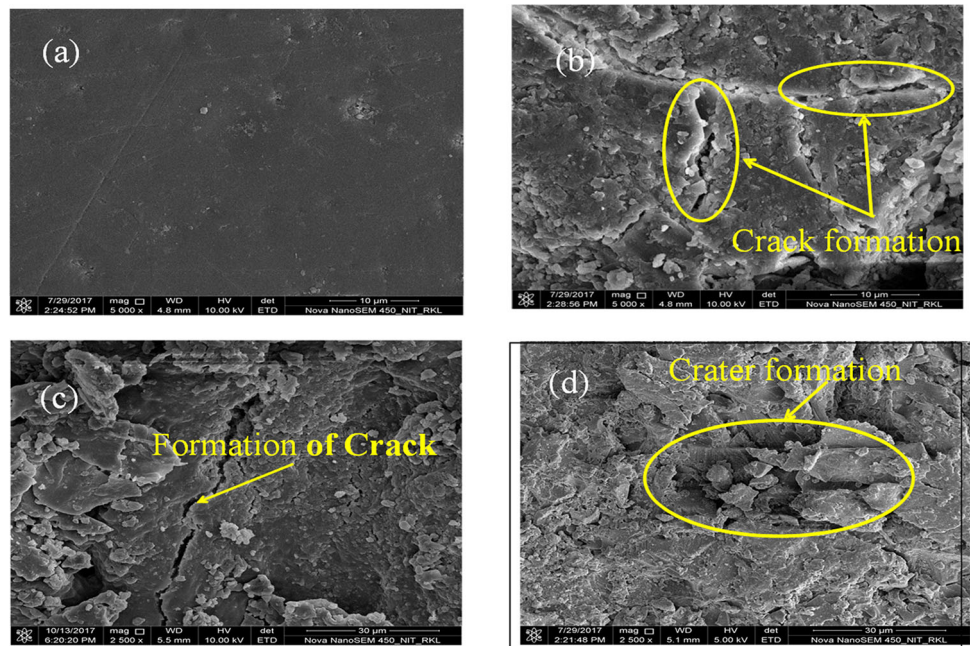
The morphology of OP4 composites at 45° impact angles and low impact velocity (48 m/s) is shown in Fig. 10b, it is observed that the formation of crater is very less but development of cracks on the surface are clearly visible. Cracks that are generated are not continuous rather moves in different directions. this is the result of hardness of OPP composite particulates energy required for plastic deformation is more in comparison to OP1 composite and hence lesser wear.

The morphology of OP4 sample at 60° impingement angle and low impact velocity (48 m/s) is presented in Fig. 10c. From figure, it is seen that cracks are generated at

the surface of the specimen but no craters are visible. This might be due to good bonding between matrix and filler material.

The SEM image of OP4 specimen at higher impact angle (60°) and velocity (i.e., 82 m/s) is presented in Fig. 10d. The craters are clearly visible at higher impact velocity due to detachment of filler materials. The energy of the erodent particle is fully transmit to the target material (OP4), which is one of the reasons for the detachment of filler materials. This is the reason for maximum weight loss of target material due to impact of erosion. It is clearly visible that there is intensive debonding

**Fig. 10** SEM images of erodent specimens (OP4) at different impact angles and velocities

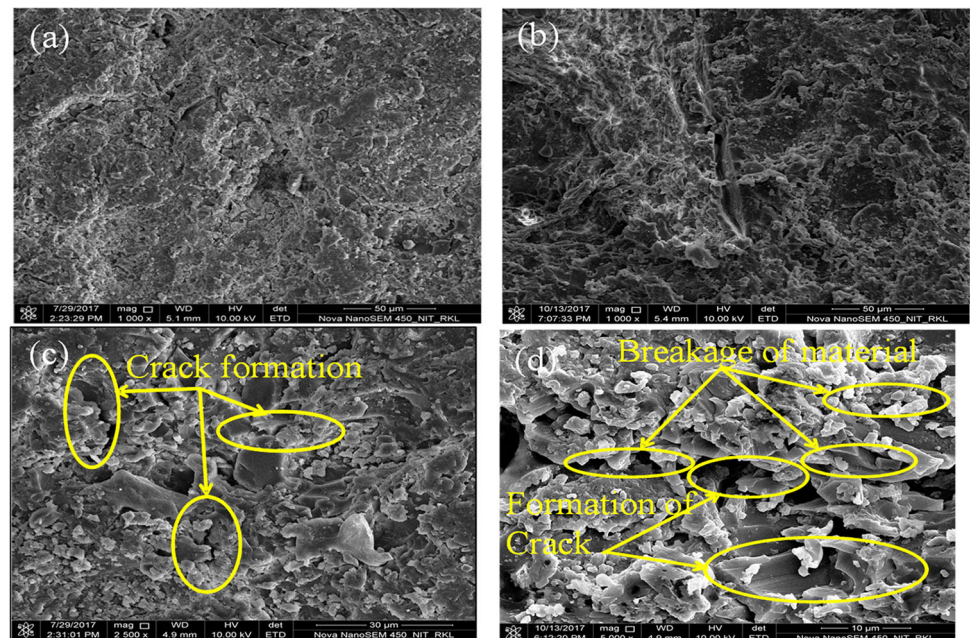


and also breakage of the fibers which are not supported by the matrix. This might have happened due to high impact velocity which is the reason for increases of temperature of the target material. So the matrix deformation was easy because of softening of the matrix material due to the temperature rise.

It is observed from Fig. 11a that the impact of erodent particle on the surface of composite specimen (OP1) is very less at low impact velocity and impingement angle 30°.

It has been observed from Fig. 11b that cracks in the surface of the specimen (OP1) is clearly visible after EW at low impact velocity (48 m/s) and impact angle (45°). However, there is no sign of pull out of filler material from the matrix material. The SEM morphology of OP1 composite at an impact velocity (72 m/s) and impact angle 45° is presented in Fig. 11c. It is noticed that the matrix is chipped off and the filler materials are clearly noticed at the beneath of the matrix layer. There is also clear sign of pull out of filler materials from the matrix as a result of which

**Fig. 11** SEM images of eroded surfaces at different OP1 composites at different impact angles and different impact velocities





cracks and multiple fractures are observed in the surface of the specimen.

The SEM surface of OP1 specimen (impact velocity (82 m/s) and 60° impact angle) is presented in Fig. 11d. The erodent particle strikes the composite surface (OP1) with full force, so there is removal of matrix material from the composite. Then the matrix is cut away and the filler materials are clearly noticeable under the matrix layer which leads to the formation of grooves on the broken part of the material. Since the amount of filler material is very less, so the interfacial adhesion between matrix and filler material is not so strong to bind the matrix material. From figure it is also observed that at higher impact the damage occurs in the matrix material due to shearing action of the filler materials. There is also separation and detachment of filler materials from the composite materials. Formation of crater, breakage of material also observed in OP1 composite material. It is due to higher velocity of erodent particle.

## Conclusions

The EW behavior of fabricated composites was studied considering various parameters such as filler percentage, impact angles and impact velocities. In this experiment silica sand act as an erodent. The subsequent outcomes are drawn from the above experiments.

- The erosion resistance of synthesized specimens enhances significantly by incorporation of OPP filler material.
- From the experimental analysis (impact of impingement angle on EW) it has been observed that the developed composite materials indicate semi ductile nature. The utmost erosion was observed in between 45° and 60° impact angle.
- The wear rate was extremely inclined toward erodent flow (impact velocity) rather than angle of impact. Thus the changes of impact velocities decides the weight change of the erodent
- The erosion efficiency ( $\eta$ ) values obtained from experimental analysis reveal that the developed composite materials exhibit semi-ductile behavior.
- SEM analysis of eroded surfaces discloses that there is high-quality bonding between matrix and filler material in the developed specimens. However the material removal in the composites materials mostly owing to microcutting and microploughing.
- From the SEM analysis it is observed that that the wear mechanism of developed specimens is greatly influenced by impact velocities. At low impact velocities, the erosive wear was influenced by fiber fracture,

matrix breakage and microcracking whereas at higher impact velocities the erosive wear mechanism was influenced by cracks, debonding, formation of craters and pits.

- From the above observation it is understood that the developed specimens may be used in different areas such as partition boards, low cost housing equipments, doors and window panels.

## References

- Adesina OT, Jamiru T, Sadiku ER, Ogunbiyi OF, Beneke LW (2019) Mechanical evaluation of hybrid natural fibre-reinforced polymeric composites for automotive bumper beam: a review. *Int J Adv Manuf Technol* 103(5–8):1781–1797
- Amiamdamhen SO, Izekor DN, Balogun AO (2016) Performance characteristics of treated kenaf bast fibre reinforced cement composite. *J Indian Acad Wood Sci* 13(2):156–160
- Barkoula NM, Karger-Kocsis J (2002) Review processes and influencing parameters of the solid particle erosion of polymers and their composites. *J Mater Sci* 37(18):3807–3820
- Bharath KN, Basavarajappa S (2016) Applications of biocomposite materials based on natural fibers from renewable resources: a review. *Sci Eng Compos Mater* 23(2):123–133
- Bhatt P, Goe A (2017) Carbon fibres: production, properties and potential use. *Mater Sci Res India* 14(1):52–57
- Bijwe J, Fahim M (2000) Tribology of high performance polymers-state of art. In: Nalawa HS (ed) *Handbook of advanced functional molecules and polymers*. Gordon and Breach, London
- Biswas S, AnivaXess P (2012) Erosion wear behaviour of bamboo/glass fiberreinforced epoxy based hybrid composites. *Int J Mech Ind Eng* 1: ISSN No. 2231–6477
- Deo C, Acharya SK (2009) Solid particle erosion of lantana camara fiber-reinforced polymer matrix composite. *Polym Plast Technol Eng* 48(10):1084–1087
- Dong G, Tang Y, Li D, Zhao YF (2018) Mechanical properties of continuous kevlar fiber reinforced composites fabricated by fused deposition modeling process. *Proc Manuf* 26:774–781
- Ferrigno TH, Katz HS, Milewski JV (1978). *Handbook of fillers and reinforcements for plastics*. In: Katz HS, Milewski JV (eds) *Van Nos trand Reinhold Co*, pp 11–58
- Foullk JA, Fuqua MA, Ulven CA, Alcock MM (2010) Flax fibre quality and influence on interfacial properties of composites. *Int J Sustain Eng* 3(1):17–24
- Fragassa C (2017) Marine applications of natural fibre-reinforced composites: a manufacturing case study. *Advances in applications of industrial biomaterials*. Springer, Cham, pp 21–47
- Gholampour A, Ozbakkaloglu T (2020) A review of natural fiber composites: properties, modification and processing techniques, characterization, applications. *J Mater Sci* 55:1–64
- Gupta A, Kumar A, Patnaik A, Biswas S (2011) Effect of different parameters on mechanical and erosion wear behavior of bamboo fiber reinforced epoxy composites. *Int J Polym Sci* 2011:592906
- Haniffah WH, Sapuan M, Abdan K, et al (2015) Kenaf fiber reinforced polypropylene composites:effect of cyclic immersion on tensile properties. *Int J Polym Sci* 2015: 872386–872387
- Harsha AP, Thakre AA (2007) Investigation on solid particle erosion behaviour of polyetherimide and its composites. *Wear* 262(7–8):807–818



- Jena H, Pradhan AK, Pandit MK (2018) Study of solid particle erosion wear behavior of bamboo fiber reinforced polymer composite with cenosphere filler. *Adv Polym Technol* 37(3):761–769
- Khan MA, Manikandan S, Ebenezer G, Uthayakumar M, Kumaran ST (2019) Solid particle erosion studies on fibre composite with egg shell as filler materials. *Int J Surf Sci Eng* 13(1):1–13
- Knoell A, Maxwell H, Bechtol C (1975) Graphite fiber reinforced bone cement. *Ann Biomed Eng* 3(2):225–229
- Kumar A, Srivastava A (2017) Preparation and mechanical properties of jute fiber reinforced epoxy composites. *Ind Eng Manag* 6(4):1–4
- Li J, Sheng XH (2010) Tribological properties of PTFE composites with addition of PA6. *Mater Technol* 25(1):30–34
- Mahesh D, Kowshigha KR, Raju NV, Aggarwal PK (2019) Characterization of banana fiber-reinforced polypropylene composites. *J Indian Acad Wood Sci* 17:1–8
- Majumdar SNG (2016) Effect of stacking sequence and hybridization on mechanical properties of jute-glass fiber composites. *Int J Perform Eng* 12(3):229–239
- Mishra P, Acharya SK (2010) Solid particle erosion of Bagasse fiber reinforced epoxy composite. *Int J Phys Sci* 5(2):109–115
- Mohammed L, Ansari MN, Pua G, Jawaid M, Islam MS (2015) A review on natural fiber reinforced polymer composite and its applications. *Int J Polym Sci* 2015:1–15
- Mohanty JR (2017) Investigation on solid particle erosion behavior of date palm leaf fiber-reinforced polyvinyl pyrrolidone composites. *J Thermoplast Compos Mater* 30(7):1003–1016
- Munde YS, Ingle RB, Siva I (2019) Effect of sisal fiber loading on mechanical, morphological and thermal properties of extruded polypropylene composites. *Mater Res Exp* 6(8):085307
- Ojha S, Raghavendra G, Acharya SK (2012) Fabrication and study of mechanical properties of orange peel reinforced polymer composite. *Cellulose* 13:0–6
- Panchal M, Raghavendra G, Prakash MO, Ojha S (2018) Effects of environmental conditions on erosion wear of eggshell particulate epoxy composites. *Silicon* 10(2):627–634
- Pani B, Chandrasekhar P, Singh S (2019) Investigation of erosion behaviour of an iron-mud filled glass-fibre epoxy hybrid composite. *Bull Mater Sci* 42(5):217
- Peças P, Carvalho H, Salman H, Leite M (2018) Natural fibre composites and their applications: a review. *J Compos Sci* 2(4):66
- Pool KV, Dharan CKH, Finnie I (1986) Erosive wear of composite materials. *Wear* 107(1):1–12
- Poursaeidi E, Niaei AM, Arablu M, Salarvand A (2017) Experimental investigation on erosion performance and wear factors of custom 450 steel as the first row blade material of an axial compressor. *Int J Surf Sci Eng* 11(2):85–99
- Prakash V, Bera T, Pradhan S, Acharya SK (2020) Potential of *Syngonanthus nitens* fiber as a reinforcement in epoxy composite and its mechanical characterization. *Cellulose* 67:1–4
- Raghavendra G, Ojha S, Acharya SK, Pal SK (2014) Jute fiber reinforced epoxy composites and comparison with the glass and neat epoxy composites. *J Compos Mater* 48(20):2537–2547
- Rajesh JJ, Bijwe J, Tewari US, Venkataraman B (2001) Erosive wear behavior of various polyamides. *Wear* 249:702–704
- Rathinavel S, Saravanakumar SS (2020) Development and analysis of poly vinyl alcohol/orange peel powder biocomposite films. *J Nat Fibers*. <https://doi.org/10.1080/15440478.2019.1711285>
- Reis JML, Amorim FC, Da Silva AHMFT, da Costa Mattos HS (2015) Influence of temperature on the behavior of DGEBA (bisphenol A diglycidyl ether) epoxy adhesive. *Int J Adhes Adhes* 58:88–92
- Rout AK, Satapathy A (2012) Study on mechanical and tribo-performance of rice-husk filled glass-epoxy hybrid composites. *Mater Des* 41:131–141
- Ruff AW, Ives LK (1975) Measurement of solid particle velocity in erosive wear. *Wear* 35(1):195–199
- Shakuntala O, Raghavendra G, Samir Kumar A (2014) Effect of filler loading on mechanical and tribological properties of wood apple shell reinforced epoxy composite. *Adv Mater Sci Eng* 2014:1–9
- Sundararajan G, Roy M, Venkataraman B (1990) Erosion efficiency—a new parameter to characterize the dominant erosion micromechanism. *Wear* 140(2):369–381
- Srivastava VK, Pawar AG (2006) Solid particle erosion of glass fibre reinforced flyash filled epoxy resin composites. *Compos Sci Technol* 66(15):3021–3028
- Sanjay MR, Arpitha GR, Naik LL, Gopalakrishna K, Yogesha B (2016) Applications of natural fibers and its composites: An overview. *Nat Resour* 7(3):108–114
- Sathishkumar TP, Satheeshkumar S, Naveen J (2014) Glass fiber-reinforced polymer composites—a review. *J Reinf Plast Compos* 33(13):1258–1275
- Santos CJE (2009) Development of fiber reinforced composite for structural applications. Submitted in partial fulfilment of course requirements for MatE B: 198
- Shahzad A (2012) Hemp fiber and its composites—a review. *J Compos Mater* 46(8):973–986
- Shimizu K, Xinba Y, Araya S (2011) Solid particle erosion and mechanical properties of stainless steels at elevated temperature. *Wear* 271(9–10):1357–1364
- Stachowiak GW, Batchelor AW, Stolarski TA (1994) *Engineering tribology*. Elsevier, Amsterdam, p 960
- Verma D, Gope PC, Shandilya A, Gupta A, Maheshwari MK (2013) Coir fibre reinforcement and application in polymer composites. *J Mater Environ Sci* 4(2):263–276
- Xie Y, Pei X, Wei S (2016) Investigation of erosion resistance property of WC-Co coatings. *Int J Surf Sci Eng* 10(4):365–374

**Publisher's Note** Springer Nature remains neutral with regard to jurisdictional claims in published maps and institutional affiliations.